Analysing of the Yarn Pull-out Process for the Characterization of Reinforcing Woven Fabrics

Ábris D. Virág[1], László M. Vas[2], Péter Bakonyi[3], Marianna Halász[4*]

[1] Budapest University of Technology and Economics, Faculty of Mechanical Engineering, Department of Polymer Engineering, Műegyetem rkp. 3., H-1111 Budapest, Hungary, viragabris@gmail.com

[2] Budapest University of Technology and Economics, Faculty of Mechanical Engineering, Department of Polymer Engineering, Műegyetem rkp. 3., H-1111 Budapest, Hungary, vas@pt.bme.hu

[3] Budapest University of Technology and Economics, Faculty of Mechanical Engineering, Department of Polymer Engineering, Műegyetem rkp. 3., H-1111 Budapest, Hungary, bakonyi@pt.bme.hu

[4] Budapest University of Technology and Economics, Faculty of Mechanical Engineering, Department of Polymer Engineering, Műegyetem rkp. 3., H-1111 Budapest, Hungary, halaszm@pt.bme.hu

Analysing of the Yarn Pull-out Process

Abstract: Our goal was to test the theoretical yarn pull-out model we developed. We examined eight glass woven fabrics from the same manufacturer. We compared the values provided by the theoretical model with the measurement results, and based on these, we determined the relationship between the length of the yarn embedded in the woven fabric and the tensile force acting on the yarn. All in all, we concluded that the model described the yarn pull-out process well; hence it can be applied to more complex woven fabric models and simulations.

Keywords: yarn pull-out, glass fibres, woven fabric, friction among fibres, modelling

1   The Principle of Yarn Pull-out

Woven fabric made of glass fibres is one of the most commonly used fibrous structures for reinforcing polymer composite products [1-4]. Regarding the 3D shape of the manufactured product, the reinforcing fabric may be assumed to be a twice-curved surface. Such great displacements and deformations significantly influence the endurance and properties of composite structures. The deformability of the reinforcing fabric mostly depends on the friction among yarns, hence it is very important to examine and analyse [5, 6]. One possible measurement method is the yarn pull-out test. Knowing the friction process between the crossing yarns, we can describe the behaviour of the fabric with models as close to reality as possible, and it provides the basis for simulation, calculation and design [7, 8].

The principle of yarn pull-out can be seen in Figure 1 [10]. During the yarn pull-out test, the woven fabric has to be clamped on both sides, then parallel to the clamps one roving is pulled from the centre line. During the pull-out process, the pull-out force and the displacement of the gripped roving end are measured [9].
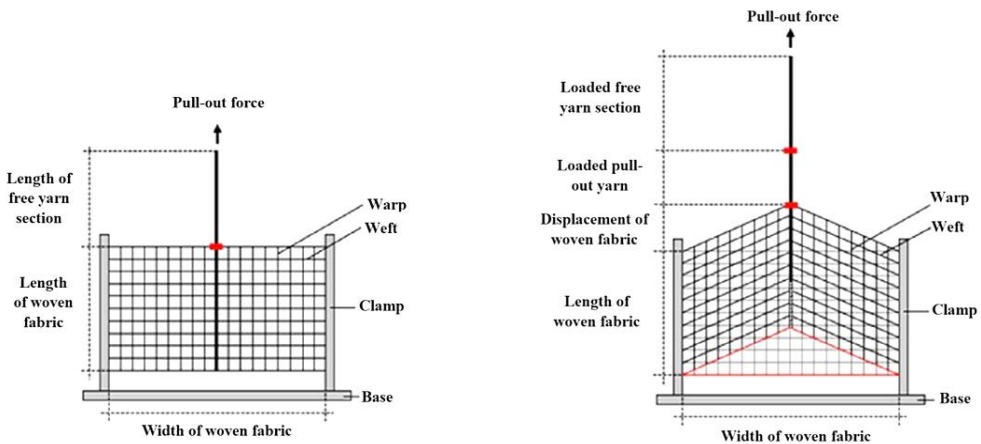

Figure 1 Principle of yarn pull-out

Measurement results are influenced by the speed of pulling out, the clamping width, the position of the clamps and the type of the clamps. It is not a standardised test; consequently it neither has a standardised implementing, nor a standardised evaluation process.

The yarn pull-out test can mainly be used to characterize the interaction among yarns. The yarn pull-out force is influenced by several parameters, for example the binding mode of the woven fabric, the pull-out length and the deformation of the fabric during pull-out [9].

The background of the processes during the pull-out has not been sufficiently explored yet, but from time to time new models are created in order to determine certain parameters. To mention a few examples: Pan and Yon [11] gave a theoretical estimation for the critical yarn length, which is the smallest length of the yarn in the fabric that breaks instead of slipping out of the fabric. Das et al. [12], Al-Gaadi [13], Prodromou and Chen [14] determined the coefficient of friction from the yarn pull-out test. There are a lot of papers dealing with the analysis and modelling of this phenomenon [10, 15-19]. Then, a simple model we elaborated will be discussed.

2   Yarn Pull-out Model

Considering the model of the yarn pull-out process, two sections can be distinguished: the yarn section, which is embedded in the woven fabric and the free yarn section, which is not built in the woven fabric (Figure 2). The yarn pull-out process is essentially a mass transport process. In the examined cases it is assumed that the yarn section in the woven fabric is inextensible and the free yarn section is deformable and linear elastic. In all cases discussed in this paper, the fundamental equation is a simple mass transport equation (1):

$$\left(l_0 + L_{w0} - l_{w0}(t)\right)\left(1 + \frac{F(t)}{K}\right) - l_0\left(1 + \frac{F(t_0)}{K}\right) = u(t) - u(t_0) \tag{1}$$

where L_{w0} [mm] is the initial unloaded length of the yarn embedded in the woven fabric, l_0 [mm] is the length of the free yarn section between the edge of the fabric and the grip, K [N] is the tensile stiffness of the yarn, $F(t)$ [N] is the measured yarn tensile force, u [mm] is the controlled displacement of the grip, and t_0 is the time point when the force reaches the value where the yarn in the fabric starts moving, hence $F(t_0)$ is the global peak value.

Fundamentally, we used two approximations. Figure 2 helps to understand this conception. The first case is based on a theoretical model (Figure 2), in which a relationship between the length of the yarn embedded in the woven fabric ($l_{w0}(t)$) and the tensile force acting on the yarn ($F(t)$) is defined as a function of time. From that the relationship between the measured quantities such as the pull-out force ($F(t)$) and the displacement of the free yarn section ($u(t)$) during the pull-out can be determined. In this case, the evaluation of the measurement results is based on a theoretical model, hence the measurement can validate the theoretical model.
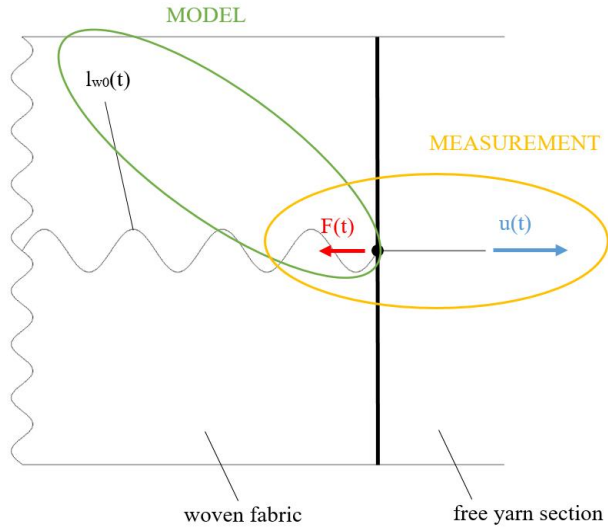
Figure 2 Conceptions of the yarn pull-out cases

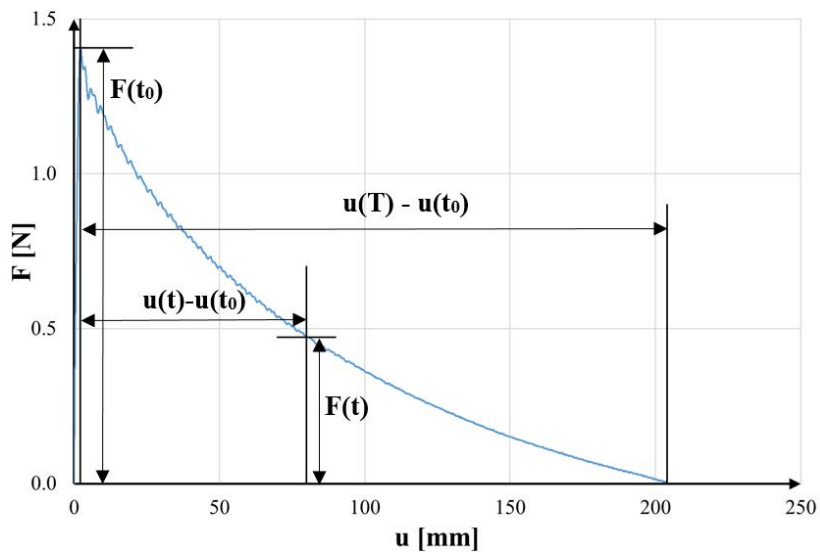Figure 3 and Figure 4 help to understand the quantities introduced above properly.

Figure 3 Yarn pull-out diagram of a typical glass woven fabric, with force and displacement type quantities from Equation (1)
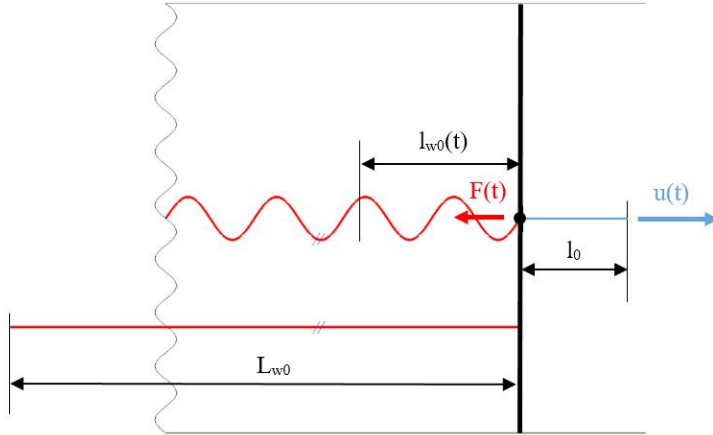
Figure 4 Explanation of the length type quantities from Equation (1)

In the second case, the measurement results are considered the basis (Figure 2), in which a fitted mathematical relationship is determined between the measured pull-out force and the measured displacement influenced by the length of the free yarn section. In the knowledge of that, the relation between the length of the yarn embedded in the woven fabric and the tensile force acting on the yarn can be assessed, which can be compared to the theoretical model. All that provides information about the applicability of the model used and how to improve that.

Different kinds of trend functions can be fitted to the measured yarn pull-out curve, but considering the monotonic decreasing character of the curve, the two most suitable trend functions proved to be the exponential and the logarithmic functions. The simplest belt friction model, the Euler-Eytelwein equation gives an exponential solution, hence in a more complex belt frictional behaviour we expected exponential process. The character of the logarithmic curve, which is the inverse of the exponential one, can be similar to the monotonic decreasing exponential curve, moreover the exponential and logarithmic curves exhibit useful robust behaviour, which means that they are not parameter sensitive when fitting them to measurements.

For the analysis and evaluation of the pull-out test results, an appropriate model is needed, which provides a mathematical relationship valid at any time point t ($0 \leq t_0 < t \leq T$) between the length of the yarn embedded in the woven fabric and the pull-out force, which is the resistance of the yarn against pulling-out. Then, an exponential theoretical model and two trends fitted to measurements are proposed and discussed.

2.1   Theoretical Exponential Yarn Pull-out Model

The model assumes an exponential relationship (exp. model) between $F(t)$ and $l_{w0}(t)$, which is similar to the Euler-Eytelwein friction equation, where $F_0>0$ is a small force loading the far end of the yarn in the fabric:

$$F(t) = F_0(e^{Bl_{w0}(t)} - 1) = F(t_0)\frac{e^{Bl_{w0}(t)} - 1}{e^{BL_{w0}} - 1} \tag{2}$$

Rearranging Equation (2) leads to:

$$F_0 = \frac{F(t_0)}{e^{BL_{w0}} - 1} \tag{3}$$

where $B>0$ is the belt friction constant, which is given by the dynamic coefficient of friction (μ_d), the cylinder radius (R) and the fraction of the contact length of the yarn ($0\leq\xi\leq1$) when belt friction is assumed:

$$B = \xi\frac{\mu_d}{R} \tag{4}$$

Expressing l_{w0} from Equation (2) and substituting it into Equation (1) leads to:

$$\left[l_0 + L_{w0} - \frac{1}{B}\ln\left(1 + \frac{F(t)}{F(t_0)}\left(e^{Bl_{w0}(t)} - 1\right)\right)\right]\left(1 + \frac{F(t_0)}{K}\frac{F(t)}{F(t_0)}\right) -$$
$$- l_0\left(1 + \frac{F(t_0)}{K}\right) = u(t) - u(t_0) \tag{5}$$

Introducing x, y and z normalized variables provides:

$$x = \frac{u(t) - u(t_0)}{u(T) - u(t_0)} \tag{6}$$

$$y = \frac{F(t)}{F(t_0)} \tag{7}$$

$$z = \frac{l_{w0}(t)}{L_{w0}} \tag{8}$$

It can be seen that x is a displacement type, y is a force type and z is a yarn length type normalized quantity.

Rearranging the right side of Equation (5) to get x from Equation (6) and using Equation (7) leads to:

$$\frac{1+\dfrac{l_0}{L_{w0}}-\dfrac{1}{BL_{w0}}\ln\left(1+y\left(e^{BL_{w0}}-1\right)\right)}{1-\dfrac{l_0}{L_{w0}}\dfrac{F(t_0)}{K}}\left(1+\frac{F(t_0)}{K}y\right)-$$

$$-\frac{l_0}{L_{w0}}\frac{1+\dfrac{F(t_0)}{K}}{1-\dfrac{l_0}{L_{w0}}\dfrac{F(t_0)}{K}}=x \tag{9}$$

The following notations are introduced:

$$a=\frac{F(t_0)}{K} \tag{10}$$

$$c=\frac{F_0}{F(t_0)}=\frac{1}{e^{BL_{w0}}-1} \tag{11}$$

$$b=BL_{w0}=\ln\left(1+\frac{1}{c}\right) \tag{12}$$

$$h=\frac{l_0}{L_{w0}} \tag{13}$$

From Equation (9), with the use of a, b, c, h, the following implicit relationship can be written for y:

$$\frac{1+h-\dfrac{\ln\left(1+\dfrac{y}{c}\right)}{\ln\left(1+\dfrac{1}{c}\right)}}{1-ha}(1+ay)-h\frac{1+a}{1-ha}=x \tag{14}$$

If a=0, Equation (14) can be simplified:

$$1 - \frac{\ln\left(1 + \dfrac{y}{c}\right)}{\ln\left(1 + \dfrac{1}{c}\right)} = x \tag{15}$$

Expressing y from Equation (15) gives a special, explicit relationship, which can be used in the case of small deformations:

$$y = c\left[\left(1 + \frac{y}{c}\right)^{(1-x)} - 1\right] \tag{16}$$

Equation (11) indicates that a small c value means strong belt friction effects, while a large c value indicates weak ones.

2.2   Exponential Trend Fitted to the Measured Curve

In the belt friction models the exponential relationship plays a significant role, as well as taking into account the monotonic decreasing character observed by testing, firstly we applied the following exponential function to the numerical approximation of the pull-out process determined by the recorded tensile force, $F(t)$, and displacement, $u(t)$:

$$F(t) = F(t_0) \frac{e^{-Bu(t)} - e^{-Bu(T)}}{e^{-Bu(t_0)} - e^{-Bu(T)}} \tag{17}$$

where considering its physical content, B is the same as in the previous case, but it has a different value.

Rearranging Equation (17) and substituting it into Equation (7) leads to:

$$y = \frac{F(t)}{F(t_0)} = \frac{e^{-Bu(t)} - e^{-Bu(T)}}{e^{-Bu(t_0)} - e^{-Bu(T)}} \tag{18}$$

Using Equation (10), (11) and (12), we get:

$$y = \frac{e^{b(1-ah)(1-x)} - 1}{e^{b(1-ah)} - 1} = \frac{e^{P(1-x)} - 1}{e^{P} - 1} \tag{19}$$

where:

$$0 < P = b(1 - ah) < \infty \tag{20}$$

Applying Equation (6), (7), (8), (10) and (13) provides:

$$(h+1-z)(1+ay) - h(1+a) = (1-ah)(1-y) \tag{21}$$

Expressing z from Equation (21) gives:

$$z = 1 + h - \frac{h(1+a) + (1-ah)(1-y)}{1+ay} = \frac{(1+a)y}{1+ay} \tag{22}$$

Substituting Equation (19) into Equation (22) leads to a relationship between z and x:

$$z = \frac{(1+a)\dfrac{e^{b(1-ah)(1-x)}-1}{e^{b(1-ah)}-1}}{1 + a\dfrac{e^{b(1-ah)(1-x)}-1}{e^{b(1-ah)}-1}} = \frac{(1+a)\dfrac{e^{P(1-x)}-1}{e^{P}-1}}{1 + a\dfrac{e^{P(1-x)}-1}{e^{P}-1}} \tag{23}$$

If $a=0$ then:

$$z = y = \frac{e^{b(1-x)}-1}{e^{b}-1} \tag{24}$$

2.3   Logarithmic Trend Fitted to the Measured Curve

As the second test function for the measured tensile force, F(t), versus displacement, u(t), relationship we selected the next logarithmic function, since as the inverse of the previously used exponential one it can also have a monotonic decreasing shape that is limited by a finite displacement where the function becomes zero similarly to the measurements:

$$F(t) = F(t_0) \frac{\ln\left(\dfrac{U}{U-(u(T)-u(t))}\right)}{\ln\left(\dfrac{U}{U-(u(T)-u(t_0))}\right)} =$$

$$= F(t_0) \frac{\ln\left(1-\dfrac{1}{U}(u(T)-u(t))\right)}{\ln\left(1-\dfrac{1}{U}(u(T)-u(t_0))\right)} \tag{25}$$

where

$$U > u(T) - u(t_0) \tag{26}$$

Rearranging Equation (25) and substituting it into Equation (7) leads to:

$$y = \frac{F(t)}{F(t_0)} = \frac{\ln\left(1 - \frac{1}{U}(u(T) - u(t))\right)}{\ln\left(1 - \frac{1}{U}(u(T) - u(t_0))\right)} =$$

$$= \frac{\ln\left(1 - \frac{1}{U}(u(T) - u(t_0))\left(1 - \frac{u(t) - u(t_0)}{u(T) - u(t_0)}\right)\right)}{\ln\left(1 - \frac{1}{U}(u(T) - u(t_0))\right)} = \qquad (27)$$

$$= \frac{\ln(1 - D(1 - x))}{\ln(1 - D)}$$

where:

$$0 < D = \frac{1}{U}\left(u(T) - u(t_0)\right) = \frac{L_{w0}}{U}(1 - ah) < 1 \qquad (28)$$

Substituting Equation (27) into Equation (22) leads to a connection between x and y:

$$z = \frac{(1 + a)\dfrac{\ln(1 - D(1 - x))}{\ln(1 - D)}}{1 + a\dfrac{\ln(1 - D(1 - x))}{\ln(1 - D)}} \qquad (29)$$

If $a = 0$ then:

$$z = y = \frac{\ln(1 - D(1 - x))}{\ln(1 - D)} \qquad (30)$$

3   Materials Examined and Their Properties

We used eight different glass woven fabrics provided by Unique Textiles to examine pull-out behaviour. Six of them can be divided into three pairs. Each pair had the same area density, but a different weave pattern. The other two had approximately the same area density, but special structures. The nominal details of the glass woven fabrics can be seen in Table 1, the structural-geometrical properties are contained in Table 2.

Table 1 Nominal details of the examined materials

Material code	Width [cm]	Weight [g/m²]	Warp density [1/cm]	Weft density [1/cm]	Warp and weft yarns code	Weave
UTE 80P	100	80	12.0	11.4	EC 9-34	Plain 1/1
UTE 80T	100	80	12.0	11.4	EC 9-34	Twill 2/2
UTE 195P	100	195	8.0	6.0	EC 13-136	Plain 1/1
UTE 195T	100	195	8.0	6.0	EC 13-136	Twill 2/2
UTE-TG 330P	127	330	N/A	N/A	N/A	Plain 1/1
UTE 306T	100	306	12.0	11.0	EC 9-68 EC 11-204	Twill 2/2
UTE 390P	100	390	7.4	6.8	EC13-272	Plain 1/1
UTE 390T	100	390	7.4	6.8	EC13-272	Twill 2/2

We performed tensile tests on the warp yarns of the glass woven fabrics, five on each material; gauge length was 50 mm and the extension rate was 100 mm/min. The tensile test properties of the examined materials can be seen in Table 3, where F_{max} is the maximal force on the tensile curve, u_{max} and ε_{max} are grip displacement and strain at maximal force, respectively. The latter is equal to the elongation at break of the yarn in this case, and finally Q means the maximal force divided by the linear density of the yarn.

Table 2 Structural-geometrical details of the examined materials

Material code	Linear density [tex]		Yarn density [1/cm]		Weight [g/m²]	Crimp [-]	Thickness [mm]
	Warp	Weft	Warp	Weft			
UTE 80P	34.70	33.70	12	11	79.74	0.004	0.07
UTE 80T	34.43	34.67	12	11	80.18	0.002	0.06
UTE 195P	137.67	136.43	8	6	187.92	0.006	0.20
UTE 195T	140.27	137.50	8	6	185.05	0.003	0.20
UTE-TG 330P	282.09	269.20	4	3	323.87	0.023	0.40
UTE 306T	69.20	203.53	9	11	307.75	0.013	0.25
UTE 390P	272.20	267.99	7	7	372.68	0.009	0.40
UTE 390T	264.18	279.52	7	7	388.11	0.008	0.35

Table 3 Tensile test properties of the examined materials

Material code	F_{max} [N]	Q [N/tex]	u_{max} [mm]	ε_{max} [-]	K [N]
UTE 80P	13.30 ±0.78	0.38 ±0.02	1.69 ±0.10	3.39 ±0.20	381.0
UTE 80T	14.63 ±0.96	0.42 ±0.03	1.77 ±0.17	3.54 ±0.34	506.5
UTE 195P	36.36 ±1.72	0.26 ±0.01	2.00 ±0.14	3.99 ±0.27	1138.1
UTE 195T	38.45 ±1.30	0.27 ±0.01	3.28 ±0.79	6.56 ±1.58	1324.0
UTE-TG 330P	121.78 ±14.19	0.43 ±0.05	5.36 ±0.31	10.73 ±0.63	1456.4
UTE 306T	32.79 ±0.78	0.47 ±0.78	1.86 ±0.22	3.72 ±0.45	956.8
UTE 390P	90.39 ±8.92	0.34 ±0.03	3.44 ±0.28	6.88 ±0.56	1108.7
UTE 390T	98.64 ±7.11	0.37 ±0.03	3.64 ±0.26	7.28 ±0.52	1107.0

4   Evaluation of the Yarn Pull-out Measurements

4.1   Testing Device

Yarn pull-out measurements were carried out with a special, multifunctional woven fabric testing device [20, 21].

This is a complex, multifunctional device, with which shear and yarn-pull out tests can be performed as well. The yarn pull-out set up can be seen in Figure 5/A [21].

The device can be connected to the tensile tester with four fastening screws. The purpose of the device is to grip the test sample properly, hence the measurement of the force and the movement of the sample are done by the tensile tester.

Before starting the test, the sample has to be clamped. The clamps are moveable sideways, but they can be fixed. The whole apparatus can be turned into a horizontal position during

the insertion of the sample, hence it makes gripping the test sample easier (Figure 5/B and 5/C) [21]. After gripping the sample, the clamps have to be set to a vertical position, while the centre line of the sample has to be positioned to the centre line of the yarn clamping unit connected to the crosshead of the tensile tester. Then a single roving from the centre line of the sample is gripped by the yarn clamping unit. After that the measurement can be started.

The size of the tested samples was 200 mm x 200 mm. The extension rate was the same as during the tensile test: 100 mm/min. The initial length of the free yarn section from the end of the fabric to the yarn clamping unit was 19.5 mm.
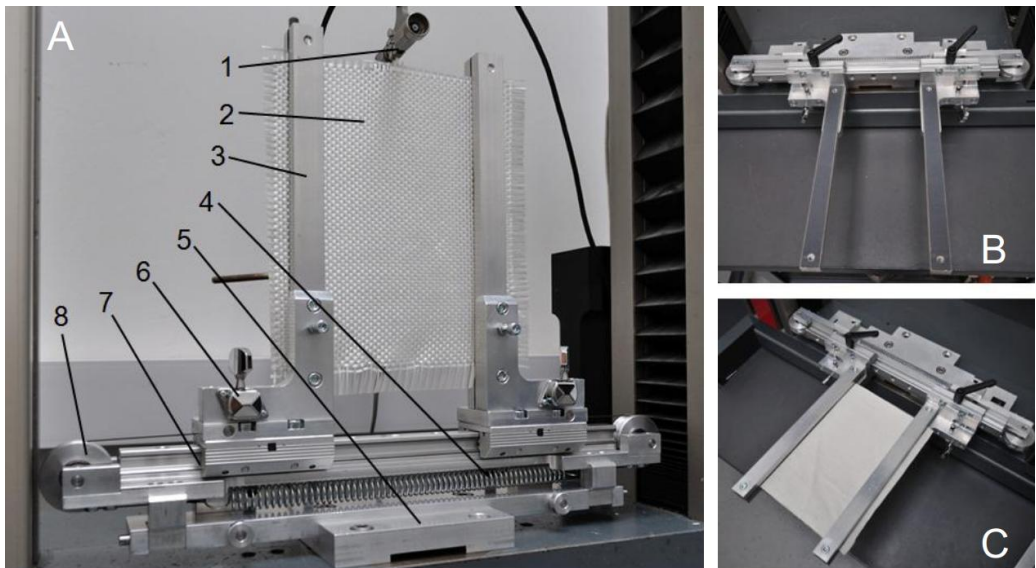
Figure 5 Multifunctional woven fabric testing device
(A: beginning of the test, B: tilted to horizontal position, C: specimen gripping, 1: clamping unit connected to the crosshead of the tensile tester, 2: test specimen, 3: clamps, 4: pretension spring, 5: motherboard, 6: gears for adjusting pretension, 7: linear bearing, 8: rollers with bearings)

4.2   Evaluation and Discussion

The process of evaluation can be seen in Figure 6. We are going to demonstrate the evaluation process with the UTE 195P material, as an example.
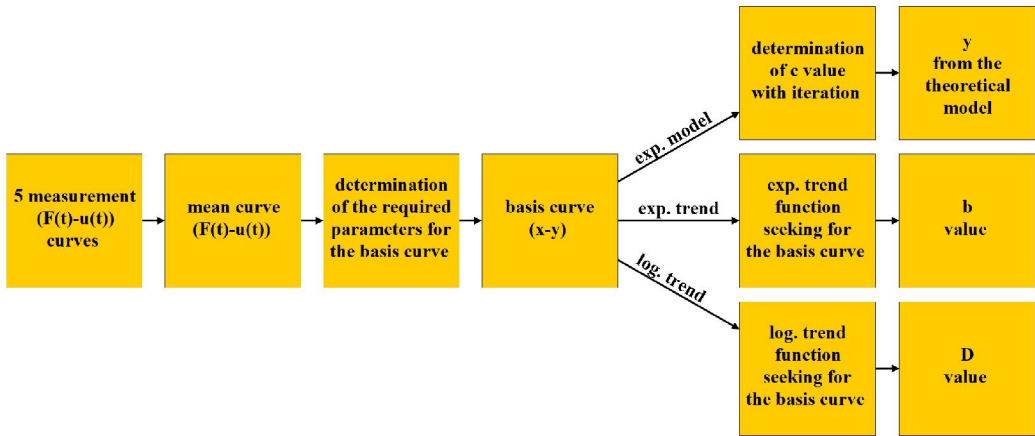
Figure 6 Process chart of evaluation

From the five measured force-displacement curves (Figure 7), a mean curve (Figure 8) was calculated. Based on that curve, we determined the quantities in Figure 2, then normalized the $u(t_0) - u(T)$ section, which is used in the evaluation, with Equation (6) and (7). This method provided a curve, which we will call the basis curve (Figure 9).
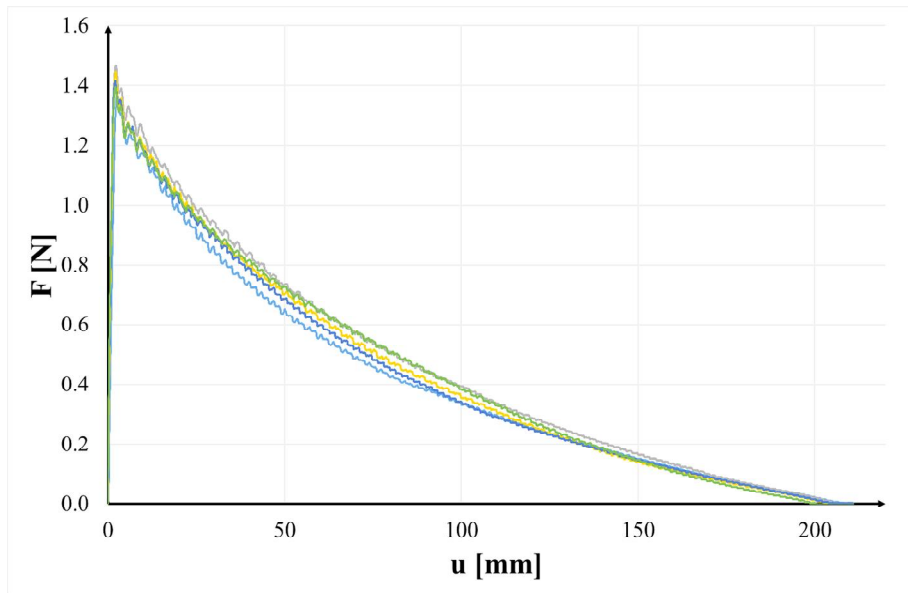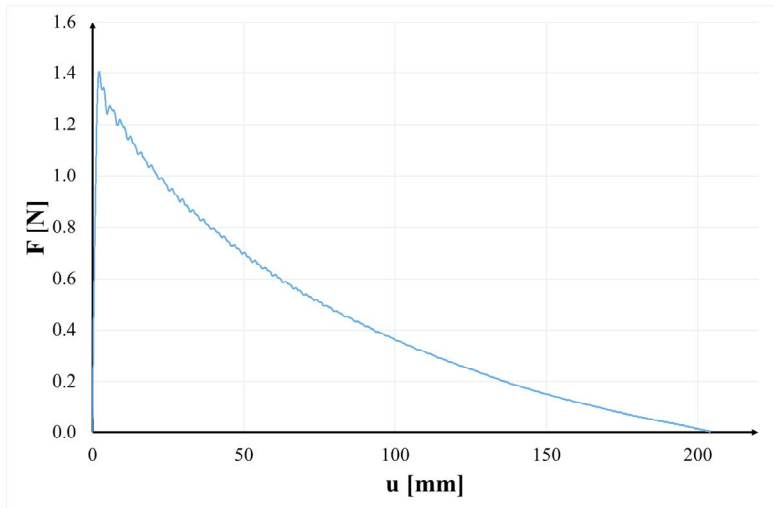

Figure 7 UTE 195P yarn pull-out curves

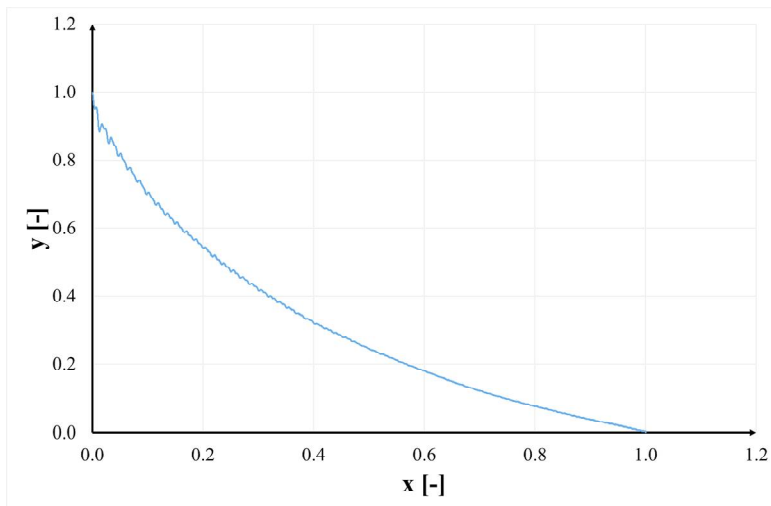**Figure 8** UTE 195P mean curve

Figure 9 UTE 195P basis curve

In the first case, according to Equation (16), the estimated y values based on the theoretical model were calculated at different values of c, thus we were able to determine the optimal value of c with iteration (Figure 10).
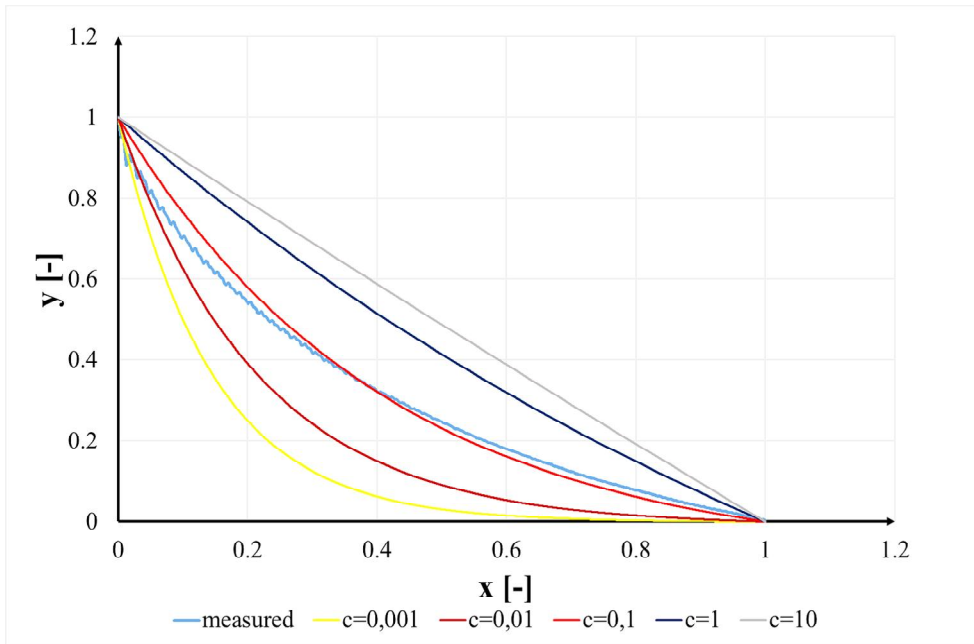
Figure 10 Calculated curves based on the theoretical model with different c values

The difference between the calculated curve based on the model and the basis curve was described with the (relative) mean squared error, which is closely related to the coefficient of determination. The optimal value of c belongs to the minimal mean squared error. The mean squared error (h_{mse}) was calculated according to Equation (31):

$$h_{mse} = \sqrt{\frac{1}{m} \sum_{i=1}^{m} (y_i - y_{est,i})^2} \qquad (31)$$

where m is the number of the measured points and y_{est} is the estimated value of y according to Equation (16). The calculated values can be seen in Table 4.

In the second case, we were looking for an exponential and a logarithmic trend function for the basis curve (Figure 11), in forms that are given by Equation (24) and (30).
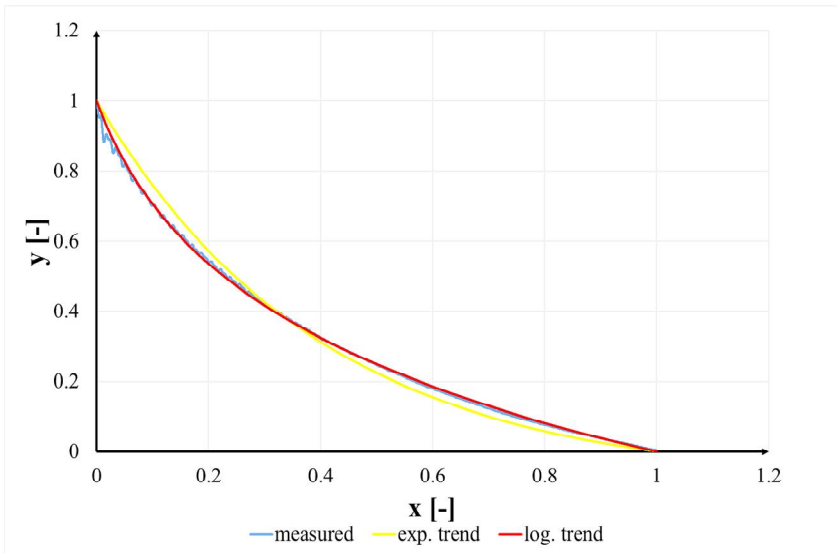
Figure 11 Fitting an exponential and a logarithmic trend to the UTE 195P basis curve

We wrote a program with Wolfram Mathematica 11.1.1., which sought trend functions in those specific forms. With the help of that, the required values b and D were given. In these cases, the fitted curves were rated by the mean squared error. The calculated values can be seen in Table 4.

Table 4 Curve fitting results

Material code	Exp. model		Exp. trend		Log. trend	
	c	h_{mse} [%]	b	h_{mse} [%]	D	h_{mse} [%]
UTE 80P	0.10	3.71	2.44	3.70	0.91	1.79
UTE 80T	0.07	2.82	2.77	2.81	0.93	0.94
UTE 195P	0.09	2.76	2.48	2.76	0.91	0.80
UTE 195T	0.13	1.84	2.16	1.83	0.88	1.05
UTE-TG 330P	0.08	4.07	2.58	4.07	0.92	1.55
UTE 306T	0.12	1.53	2.20	1.51	0.88	1.81
UTE 390P	0.19	2.34	1.81	2.31	0.84	1.05
UTE 390T	0.10	1.16	2.36	1.09	0.90	1.72

According to Table 4, the (relative) mean squared error (h_{mse}) is below 4.1% in every case hence both the exponential model and the two trends can be used for describing the measured process mathematically. Moreover, in the case of the logarithmic trend it is smaller than 2% meaning a somewhat better quantitative fitting. Nevertheless, applying the

exponential model or trend, the h_{mse} for the twill fabrics (1.09-2.82) is significantly smaller (by ~0.9-2.5%) than that for the plain ones (2.31-4.07), on the other hand the h_{mse} for the twill fabrics exhibit consistent decrease with the increasing area density. These may be explained by the structural difference since the twill weave pattern contains less transitional places than the plain one, otherwise the larger area density is realized by smaller warp yarn density which may lead to more determined „belt-friction-like" behaviour. However, fitting the logarithmic trend leads to smaller h_{mse} values and smaller differences between the plain and twill h_{mse} values otherwise the sign of the latter is positive only for the fabric of least area density. Thus, we may say that, in the examined cases, the belt friction based exponential description, although it provides somewhat larger fitting error, can be more sensitive to the structural differences than the logarithmic one.

5 Conclusions

We created a simple theoretical yarn pull-out model and two approximations. To examine their applicability, we performed yarn pull-out tests on eight different glass woven fabrics and evaluated the measurement results in order to analyse and model the yarn pull-out process. Although the theoretical model does not take the decaying periodicity of the yarn pull-out curve into consideration, with the appropriate value of c the proposed theoretical model can describe the character of the pull-out curve and the exponential and logarithmic approximations can contribute to further modelling and development. Their applicability is confirmed by the fact that the deviation between the results of models and measurements was less than 5% in all cases. In addition, when the deformation is small enough or the tensile stiffness of the yarn is large, the relationship between the pulling-out force and the length of the yarn gripped in the fabric can be approximated by a homogeneous linear function in both the exponential and the logarithmic trends. This may be crucially important in the case of large tensile modulus such as that of the carbon fibers.

Nanotechnology research area of the Budapest University of Technology and Economics (BME FIKP-NANO).

References

1. T. Szmechtyk, N. Sienkiewicz, and K. Strzelec, *Express Polym Lett*, **12**, 640 (2018).

2. G. Fredi, A. Dorigato, and A. Pegoretti, *Express Polym Lett*, **12**, 349 (2018).

3. M. W. Kim, S. H. Kwon, H. Park, and B. K. Kim, *Express Polym Lett*, **11**, 374 (2017).

4. L. Kovács, and G. Romhány, *Period Polytech Mech*, **62**, 158 (2018)

5. C. Budai, and L. Kovács, *Period Polytech Mech*, **61**, 266 (2017).

6. H. Al-Maliki, and G. Kalácska, *Period Polytech Mech*, **61**, 303 (2017).

7. G. Bojtár, B. M. Csizmadia, and J. Égert, *Acta Polytech Hung*, **14**, 47 (2017).

8. L. M. Vas, F. Göktepe, P. Tamás, M. Halász, D. Özdemir, L. Kokas-Palicska, and N. Szakály, *Acta Polytech Hung*, **10**, 79 (2013).

9. M. Halász, *Magyar Textiltechnika*, **69**, 29 (2017).

10. K. Bilisik, *Compos Part A-Appl S*, **42**, 1930 (2011).

11. N. Pan, and M.-Y. Yoon, *Text Res J*, **63**, 629 (1993).

12. S. Das, S. Jagan, A. Shaw, and A. Pal, *Compos Struct*, **120**, 129 (2015).

13. B. Al-Gaadi, and M. Halász, *Fiber Polym*, **14**, 804 (2012).

14. A. G. Prodromou, and J. Chen, *Compos Part A-Appl S*, **28**, 491 (1997).

15. Z. Dong, and C.T. Sun, *Compos Part A-Appl S*, **40**, 1863 (2009).

16. E. Tapie, Y. B. Guo, and V. P. W. Shim, *Int J Solids Struct*, **80**, 212 (2016)

17. G. Nilakantan, and W. Gillespie Jr., *Compos Struct*, **101**, 215 (2013)

18. D. Zhu, C. Soranakom, B. Mobasher, and S. D. Rajan, *Compos Part A-Appl S*, **42**, 868 (2011).

19. X. B. Zhang, H. Aljewifi, and J. Lic, *Procedia Materials Science*, **3**, 1377 (2014)

20. K. Molnár, M. Halász, and L. M. Vas: Determination of Shear Properties and Yarn Pull-out Behavior of Textiles by Novel Apparatus, in Proceedings of *4th IJCELIT Conference*, Budapest, Hungary, 2013

21. K. Molnár, M. Halász, and L. M. Vas: Apparatus for measuring the shear properties of reinforcements, in Proceedings of *4th ITMC Conference*, Roubaix, France, 2013